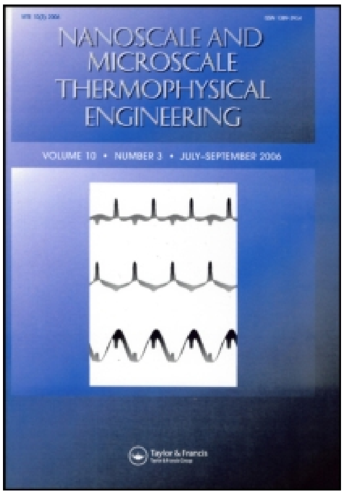

Nanoscale and Microscale Thermophysical Engineering
Publication details, including instructions for authors and subscription information:
http://www.informaworld.com/smpp/title~content=t713774103

Valveless Small Gas Pump

Xiao-Bing Luo[a]; Hye-Jung Cho[b]
[a] School of Energy & Power Engineering, Huazhong University of Science & Technology, Wuhan, China [b] Energy Lab, Samsung Advanced Institute of Technology, Korea

To cite this Article Luo, Xiao-Bing and Cho, Hye-Jung(2006) 'Valveless Small Gas Pump', Nanoscale and Microscale Thermophysical Engineering, 10: 2, 83 — 94
To link to this Article: DOI: 10.1080/10893950600642933
URL: http://dx.doi.org/10.1080/10893950600642933

Nanoscale and Microscale Thermophysical Engineering, 10: 83–94, 2006

ISSN: 1556-7265 print / 1556-7273 online
DOI: 10.1080/10893950600642933

VALVELESS SMALL GAS PUMP

Xiao-Bing Luo
School of Energy & Power Engineering, Huazhong University of Science & Technology, Wuhan, China

Hye-Jung Cho
Energy Lab, Samsung Advanced Institute of Technology, Korea

In this article, a small valveless gas pump based on a synthetic jet actuator is developed. Instead of a check or active valve, a special flow control structure in consideration of synthetic jet characteristics is designed to realize valve function. A small-sized prototype of this pump is presented. Numerical simulation by using a simplified fluid model is conducted. The results reveal that the present small valveless pump can achieve gas pumping with large flow rate. However, it is also noted that in one operation cycle, there exists a period when a small amount of backflow appears.

KEY WORDS: valveless gas pump, synthetic jet actuator, numerical simulation

INTRODUCTION

Small or micro gas pumps are widely used in medical, automotive, gas sampling, gas analysis, and miniature direct methanol fuel cell (DMFC), micro cooling, etc. [1–3].

A number of small pump designs have been proposed in the last two decades [4,5]. In these designs, mechanical pumps with vibrating membrane attract more attention because of their high feasibilities in applications. Usually they consist of two key parts: a small actuator and a flow direction control component. It is easy to differentiate the two parts from the structure. As to the small actuator, common principles include piezoelectric, thermo-pneumatic, electro-static, electro-magnetic, and shape memory actuation. For the flow direction control part, a valve is often adopted. The appearance of the valve makes the device response slow. Furthermore, a movable valve brings some problems such as material fatigue, high-pressure drops, performance instability, or invalidation, which consequently influence the life of a small pump. Otherwise, slight fluid leaks still exists in most of valve pump, which reduce the pumping flow rate.

To overcome or partly overcome the problems brought by valves, several so-called valveless mechanical micro pumps were presented. The most famous one is the diffuser/nozzle-based fluid pump proposed by Stemme and Stemme [6]. It uses

Received 16 August 2004; accepted 15 November 2005.
This paper was presented at the Micro/Nanoscale Energy Conversion Transport 2004; August 9–12 at Inje University, Korea.
Address correspondence to Xiao-Bing Luo, School of Energy & Power Engineering, Huazhong University of Science & Technology, Luoyu Road 10137#, Wuhan, China 430074. E-mail: luoxb@mail.hust.edu.cn

NOMENCLATURE

t	time,
$\bar{u}$	streamwise component of velocity, m/s
U_0	maximal averaging velocity of jet outlet, m/s

Greek Symbols

η	cross-stream direction
ω	angle frequency of actuator, rad/s
ξ	streamwise direction

diffuser/nozzle elements that have direction-dependent flow resistance to replace the conventional check valve. A maximum achievable forward-backward flow ratio of 2.23 is reported for this pump. Another kind of valveless micro pump using heat-based flow rectification principle is also developed [7]. In this pump, the flow resistance difference in narrow channels caused by the temperature dependence of liquid viscosity is utilized to get the valve effect, and its pumping function and ability of bi-directional pumping were confirmed by experiment. Tsai and Lin [8] demonstrate a creative valveless micropump actuated by a thermal bubble. A maximum 5 μL/min is observed by experiment when the driving frequency is 250 Hz at 10% duty cycle with 1 W power consumption. Such a mechanism provides a novel method for microfluidics applications. For the above-mentioned valveless pumps, their constructions are relatively simple compared to those pumps with check or active valves. As a result, the reliability of these valveless pumps will increase. Because of this, although the flow rectification for valveless pumps is not perfect, they are still quite attractive.

In this article, a novel valveless small gas pump based on a synthetic jet actuator [9–11] is presented. Instead of a mechanical check valve, a special flow control structure in consideration of synthetic jet characteristics is adopted to realize flow rectification. Numerical simulation and analysis are carried out to prove its principle. The results demonstrate that it can be used to realize gas delivery with large flow rate.

DESIGN AND PRINCIPLE

Since synthetic jet is an important concept for present pump, it will be first introduced here. A synthetic jet has emerged as a versatile small actuator with various potential applications such as separation and turbulence control, thrust vectoring, micro mixing, and cooling. Figure 1 illustrates the schematic of a synthetic jet. When fluid is driven out of cavity, a shear layer is formed at the orifice, then rolls up to form vortex rings. When the membrane moves down to pull fluid into the cavity, the vortex rings have moved far away from the orifice so that they are unaffected by the fluid motion at the orifice. These vortex rings finally form a turbulent jet after undergoing instability and breaking down. As the result of the periodic movements of the membrane, a quasi-steady jet flow is established while the net mass in or out of the orifice is zero, which is the essential difference compared with normal jet.

Figure 2 shows one embodiment of the present pump concept, which is based on precision fabrication. It includes three parts: a polyhedron cavity with a gas outlet, a central orifice plate with some orifices, and a synthetic jet actuator part. As shown in Figure 2, the central orifice plate includes two fresh gas entry orifices and one synthetic jet orifice, with the two fresh gas entry orifices symmetrically distributed in both sides of the jet orifice. The synthetic jet actuator consists of one cavity and a planar circular electromagnetic actuator. The cavity is positioned below the jet orifice of the central

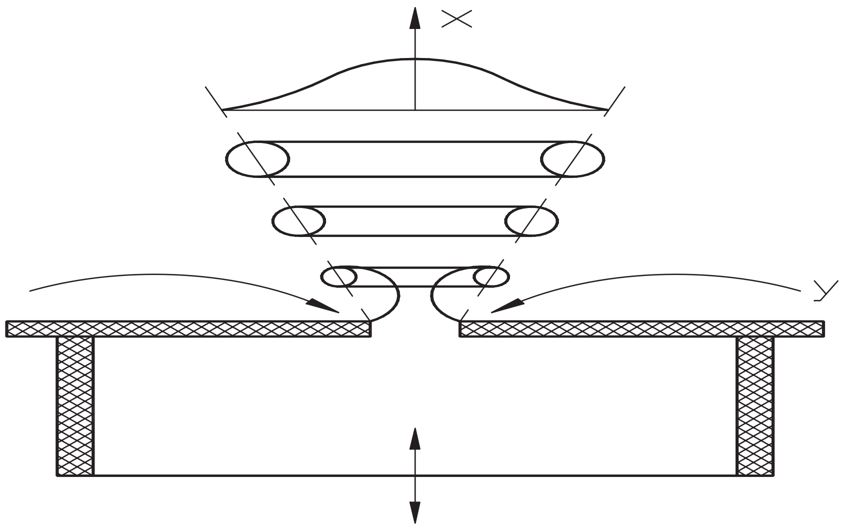

Figure 1. The schematic diagram on cross-sectional view of synthetic jet.

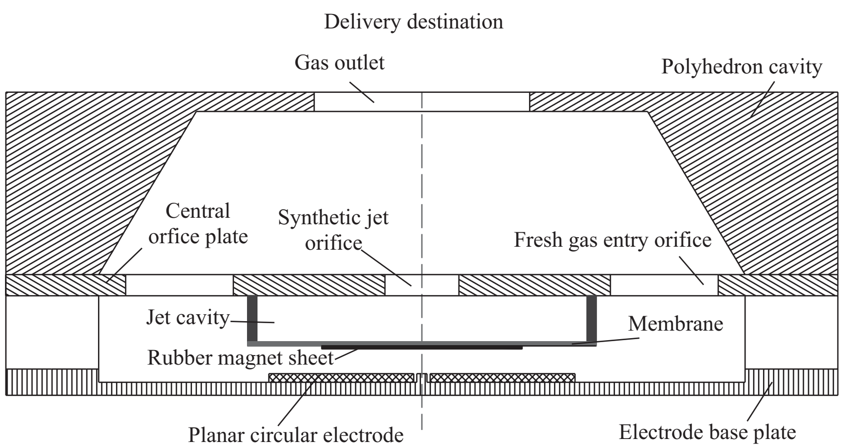

Figure 2. The small-sized valveless gas pump structure.

orifice part. A vibration membrane attached with a rubber permanent magnet sheet is bonded to the cavity, and the magnet sheet couples with the planar circular coil in the electrode base plate to produce electromagnetic force. The periodic magnetism will drive the membrane into vibration and correspondingly synthetic jet forms.

For the present pump, obviously, the fabrication difficulty focuses on the synthetic jet actuator. Glezer et al. [9,11] have demonstrated several micro fabrication designs for a synthetic jet actuator. Therefore, the concept of the present gas pump can be realized by other actuator and micro fabrication, and it is not limited to electromagnetic actuator and conventional precision machining as demonstrated in Figure 2. This means that the concept of the present pump can be used for micro pump design.

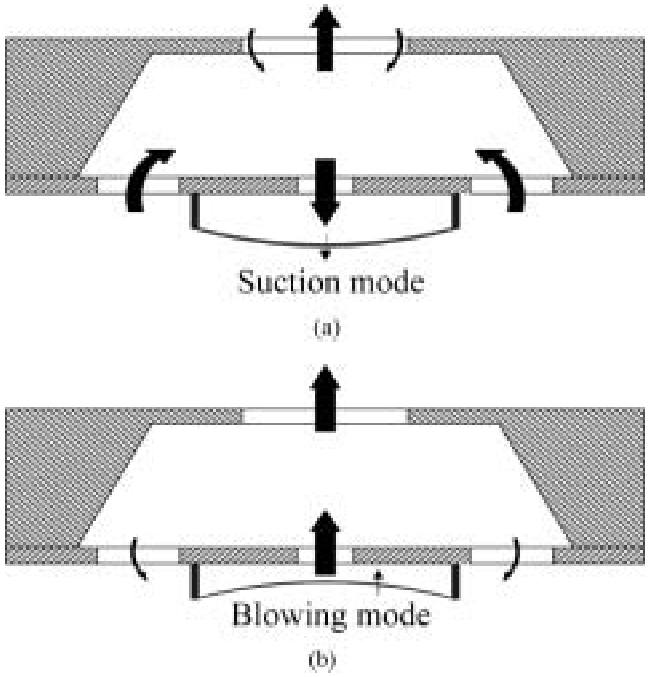

Figure 3. (a) Typical flow schematic in suction mode of gas pump. (b) Typical flow schematic in blowing mode of gas pump.

The basic principle of the present small pump is illustrated in Figure 3. The direction and size of the arrows in Figure 3 clearly display the flow direction and flow rate magnitude. The pump operation cycle constitutes of two half periods: suction stroke and blowing stroke. In Figure 3 (a), the synthetic jet actuator is in suction mode; at this time, the main stream of the synthetic jet still exists, and it flows out to the delivery destination through the gas outlet. Synchronously, much gas is imbibed into the synthetic jet cavity, most of which comes from the fresh gas orifice, and a small amount of which comes from the gas outlet, as the arrows show in Figure 3 (a). Figure 3 (b) demonstrates the blowing mode of the present gas pump. During this period, gas flows out from the synthetic jet cavity, most of it flowing into the delivery destination through the gas outlet, and a small amount returning to the gas source through the fresh gas entry orifice. Integrating the above two periods, for the present small gas pump, it is easily found that in one cycle there is net flow rate from the fresh gas source to gas delivery destination. This pump does not have any conventional check or active valves, so it is a kind of valveless design.

NUMERICAL SIMULATION

The design demonstrated in Figure 2 is a coupled mechanical/electrical/fluid flow model, it is very difficult to take into account all flow, mechanical, and electrical parameters in simulation. In order to accurately simulate the flow characteristics and delivery flow rate, a simplified model shown in Figure 4 is adopted. Obviously, the

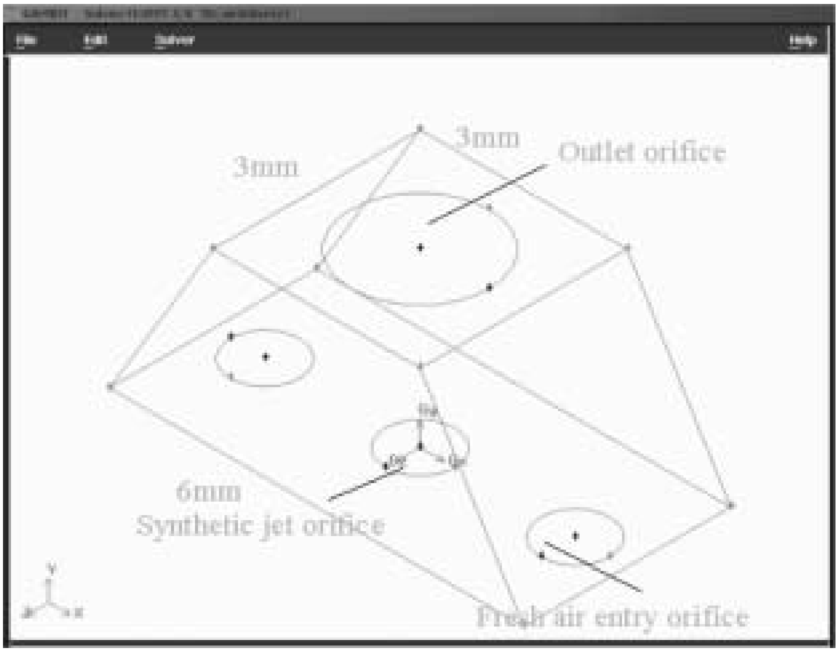

Figure 4. Simplified CFD model of present valveless gas pump.

boundary condition at the synthetic jet orifice is the key factor for getting the proper flow information of the present pump.

Air is the calculation material for the present simulation. The unsteady, three-dimensional, incompressible, Reynolds-averaged Navier-Stokes (RANS) equations are solved. A standard κ-ε turbulence model is used. It has been proven that the simulation results by using the above method can achieve good agreement with experiment results [12–14]. Commercial code FLUENT 6.1 is used here.

The corresponding boundary conditions of the present model are as follows. For the synthetic jet orifice, it belongs to the blowing/suction boundary condition. Karl et al. [12] proves that the following equation can simulate the synthetic jet orifice effectively.

$$\overline{u}(\xi = 0,\eta,t) = U_0 f(\eta) Sin(\omega t) \tag{1}$$

where ξ denotes the streamwise direction, η denotes the cross-stream direction, $\bar{u}$ is the streamwise component of velocity, and ω is the angle frequency of the actuator. Because the orifice size is very small, the orifice velocity can be regarded as the same along the cross-stream direction, which means that $f(\eta) = 1$, thus Eq. (1) can be rewritten as,

$$\overline{u}(\xi = 0,\eta,t) = U_0 Sin(\omega t) \tag{2}$$

For the fresh gas entry orifice and outlet orifice, the natural pressure boundary conditions are adopted in simulation.

In the computations, the diameters of synthetic jet and fresh gas entry orifice are 1 mm and the outlet orifice diameter is 2 mm. The height of the polyhedron cavity is 2.5 mm; other main dimensions can be found from Figure 4. Based on the experiments of a synthetic jet actuator [10,11,13,15,16], the orifice averaging maximum velocity U_0 is assumed as 10 m/s and the actuator's frequency is 1000 Hz.

The convergence studies on grids, time steps in one cycle, and maximum iteration times in one time step are conducted before the calculation. They are refined until the flow field changes by 0.8%. Finally, 16,542 grids and 20 time steps per cycle are used in the simulation. The residual control of the continuity equation is 0.01%.

ANALYSIS AND DISCUSSION

Figures 5 and 6 exhibit the flow field distribution for $Z = 0$ section at time $t = 0.4T$ when actuator is working in blowing mode. Figure 5 denotes the velocities at different positions, especially at the boundaries. In Figure 5, the abscissa denotes the position along the X axis and the ordinate denotes the Y axis velocity of air. Air velocities at the synthetic jet orifice, fresh gas entry orifices and outlet orifice are denoted by different points marked in Figure 5. For other points that are not noted

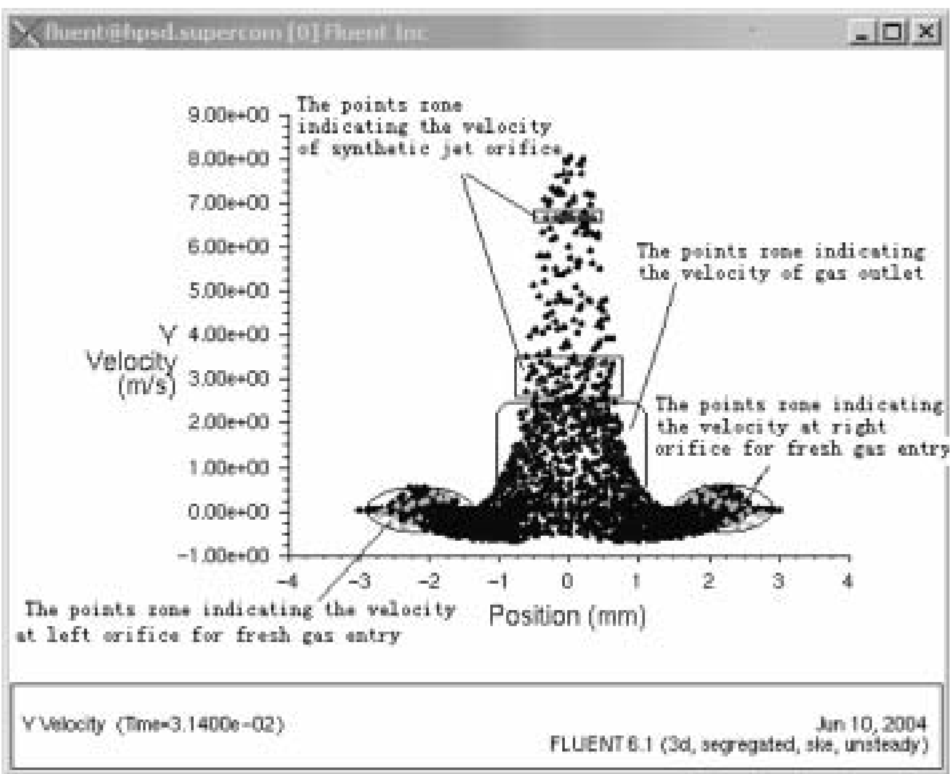

Figure 5. Flow field distribution for $Z = 0$ section in blowing stroke ($t = 0.4T$).

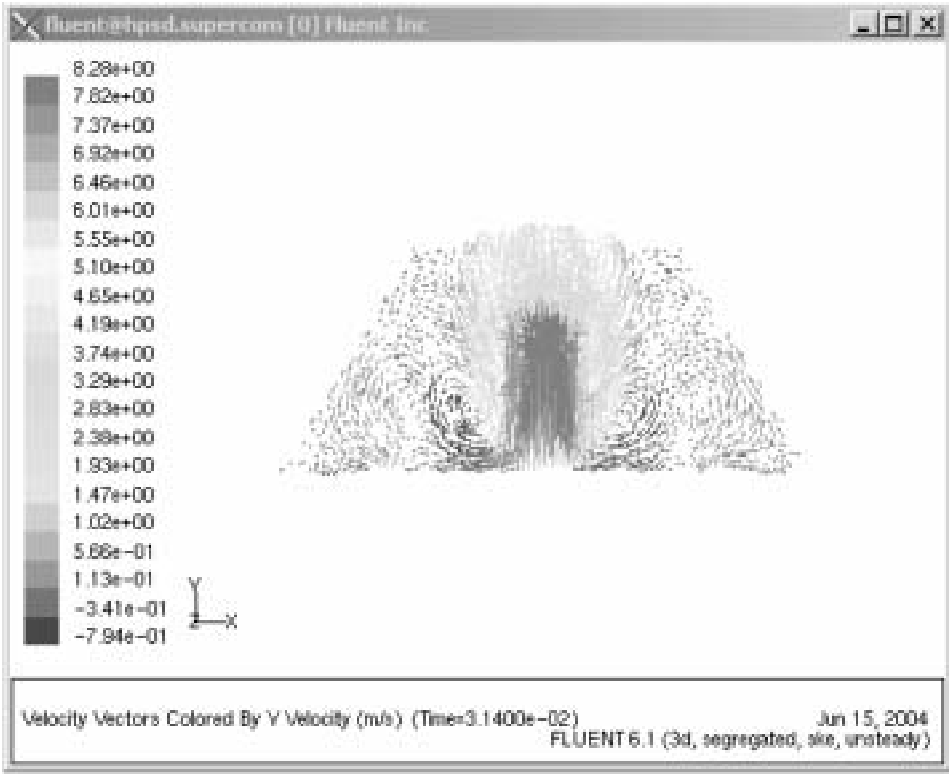

Figure 6. Flow pattern for $Z = 0$ section in blowing stroke ($t = 0.4T$).

in Figure 5, they denote the velocities inside the polyhedron cavity. It can be seen from Figure 5 that the velocities at the synthetic jet orifice are positive, which means that the synthetic jet actuator is working in blowing mode air flows into the polyhedron cavity from the synthetic jet cavity through the synthetic jet orifice. The fact that the velocities at gas outlet orifice are positive in Figure 5 also demonstrates that air in the polyhedron cavity flows out from the outlet orifice to the delivery destination. For air velocity at both fresh gas entry orifices, it is clear that a small amount of air in the polyhedron cavity flows out from the fresh gas entry orifice since some points indicate negative velocity. According to the above discussion, it can be found that in the blowing stroke, most of the air coming from the synthetic jet cavity is delivered to its destination from the outlet orifice, and a small amount of it returns to delivery source from the fresh gas entry orifice.

Figure 6 shows the flow pattern in $Z = 0$ plane at time $t = 0.4T$. It clearly shows that most of the air from the synthetic jet orifice is delivered to outside from the outlet orifice. A very small amount of air flows out from the fresh gas entry orifice to return to gas sources. As demonstrated in many other simulations and experiments on synthetic jets, here, two obvious vortexes are also observed near the synthetic jet orifice in Figure 6.

Figures 7 and 8 exhibit the flow field distribution for $Z = 0$ section in suction stroke at time $t = 0.6T$. Negative air velocity at the synthetic jet orifice denoted in

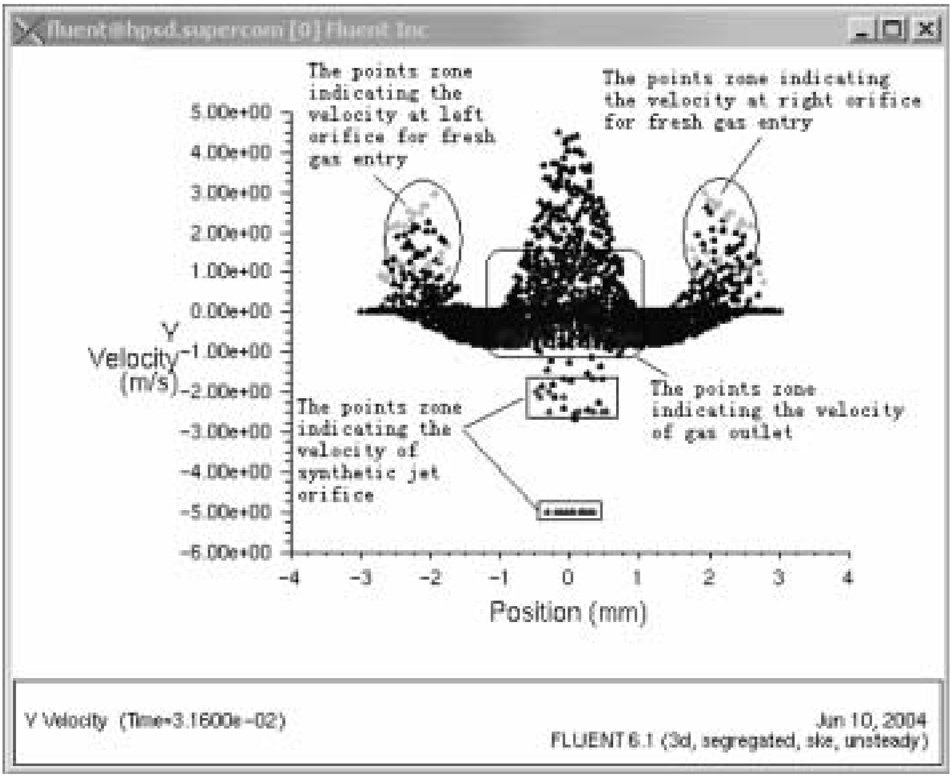

Figure 7. Flow field distribution for $Z = 0$ section in suction stroke ($t = 0.6T$).

Figure 7 demonstrates that the pump is in suction stroke. Some air in the polyhedron cavity is imbibed into the synthetic jet cavity. The positive air velocity at the fresh gas entry orifice denoted in Figure 7 shows that air from the delivery resource flows into the polyhedron cavity. It is also noted from Figure 7 that the jet flow still exists in suction stroke, and some air in the polyhedron cavity flows out to the delivery destination through the outlet orifice. Figure 8 clearly reveals the flow pattern at $Z = 0$ section in suction stroke. It can be seen that much air from the delivery source flows into the polyhedron cavity. Some air in the polyhedron cavity is imbibed into the synthetic jet cavity from the jet orifice, some of which flows to the delivery destination from the outlet orifice by the form of jet. In Figure 8, two vortexes still can be observed; however, compared with those in Figure 6, they have moved a little far from the synthetic jet orifice.

Considering the above two strokes together, it can be seen that in one cycle, fresh air from the gas delivery source is imbibed into the synthetic jet cavity and most of the air is delivered into the delivery destination by the form of jet, and very small amount of air returns to the delivery resource. Here it should be noted that for the present pump, gas delivery to destination exists during the whole working period, but its flow rate in suction stroke is much lower than that in blowing stroke.

Figure 9 shows the dependence of flow rate on time in one cycle. The averaging flow rate flowing through each boundary is marked by the dashed line. All three

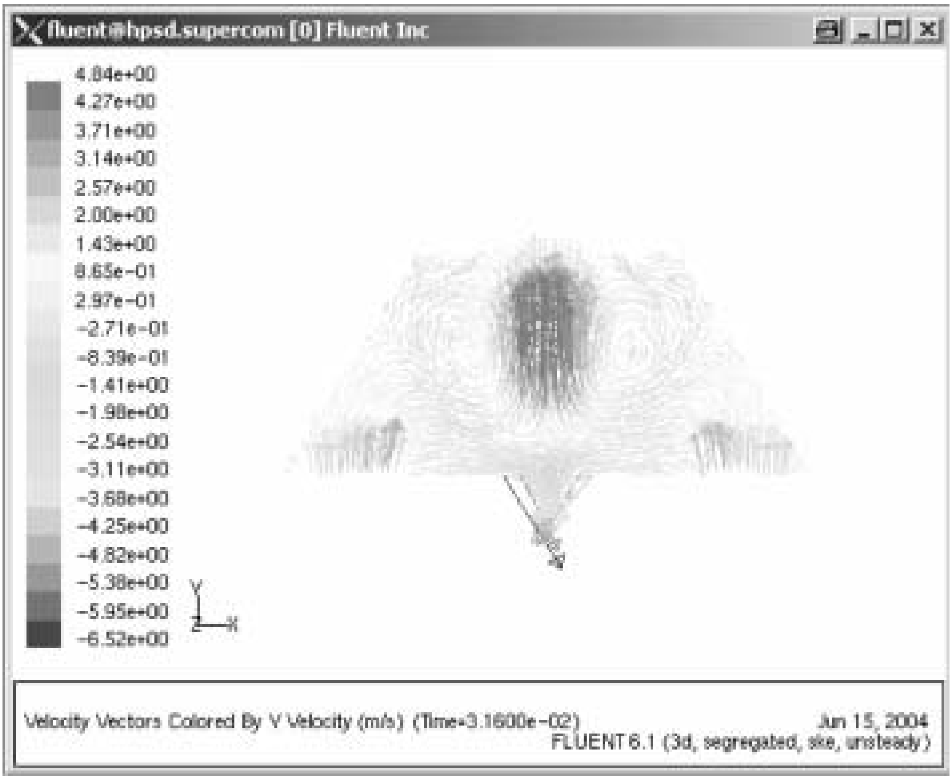

Figure 8. Flow patterns for $Z = 0$ section in suction stroke ($t = 0.6T$).

curves are sine types. It can be seen that in one cycle, the net flow rate at the synthetic jet orifice is 0, the averaging flow rate into the system from the fresh gas entry orifice is 87 mL/min, and the averaging flow rate flowing out of the system to delivery destination from the outlet orifice is also 87 mL/min. The above data demonstrates that in one cycle, air from the fresh gas entry orifices enters into the system and is finally delivered out to the destination from the outlet orifice; the synthetic jet cavity and polyhedron cavity just function as a temporary container. Therefore, it can be concluded that the present pump can realize gas delivery and fulfill the basic function of a miniaturized pump. Since its structure does not use any check or active valves, it is a kind of valveless pump. Figure 10 demonstrates the averaging net flow rate of the present gas pump. From Figure 10, it is noted that in one operation cycle, there exists $0.38T$ period (from $0T$ to $0.38T$). During this period, a small amount of backflow appears. Therefore, the present small gas pump can be used in the applications that do not strictly require any leakage such as the air delivery device for DMFC (direct methanol fuel cell).

CONCLUSIONS

A kind of small valveless gas pump is presented in this article. Such a concept can also be used for micro pump design. It employs a synthetic jet

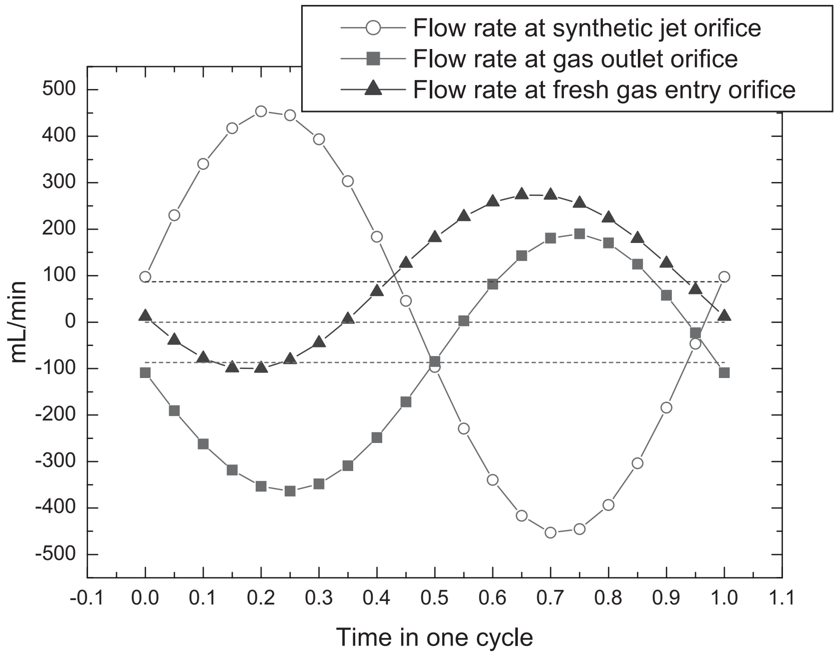

Figure 9. Flow rate in one cycle for different orifices. Positive value: flow into polyhedron cavity; negative value: flow out of polyhedron cavity.

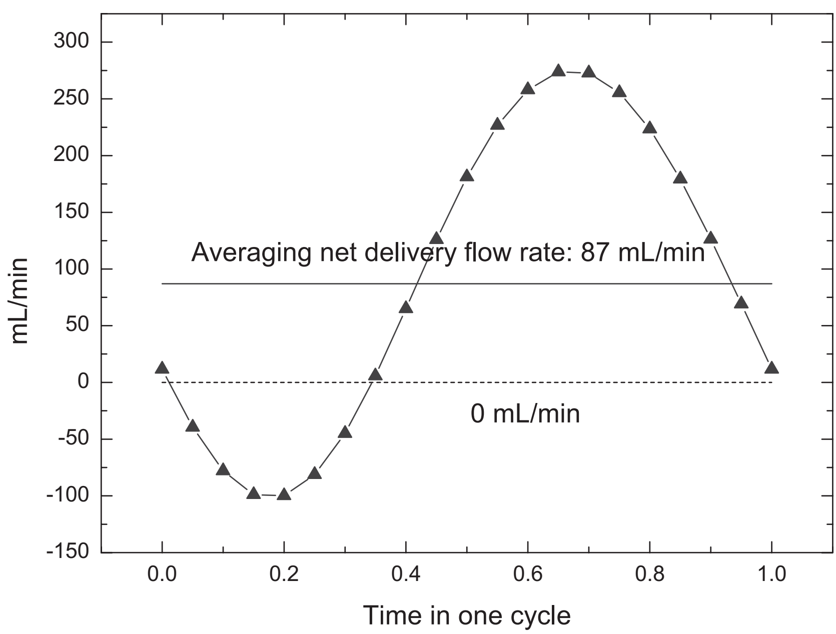

Figure 10. Averaging delivery flow rate for present gas pump.

actuator and a special structure to realize the flow control and does not need check or active valves. The pump has two operation processes in one cycle. When on suction stroke, much gas from the delivery source is imbibed into the pump. Meanwhile, some gas in the pump cavity is delivered to the pumping destination by the form of synthetic jet. When on blowing stroke, most of the gas in the pump cavity flows out and enters into the pumping destination and a small amount of gas returns to gas source, which means that there is gas leakage for the present pump. By the reciprocal running of the above two strokes, gas transportation from the delivery source to the pumping destination can be realized. Numerical simulation and analysis about a small-sized prototype are also conducted in this article. The results show that the flow rate of the pump can reach to 87 mL/min for air if the actuator's frequency is 1000 *Hz* and maximum averaging velocity at synthetic jet orifice is 10 m/s.

REFERENCES

1. Http://www.sensidyne.com/MiniatureAirPumps.php.
2. M.J. Tsai, S.C. Lo, R.T. Chen, and T.C. Wu, Ozone Generator Having Micro Pump, U.S. patent number 5908603, 1999.
3. J.W. Bostaph, C.R. Koripella, and A.M. Fisher, Direct Methanol Fuel Cell System Including an Integrated Methanol Sensor and Method of Fabrication, U.S. patent number 6696189, 2004.
4. S. Shoji and M. Esashi, Microflow Devices and Systems, *Journal of Micromechanical Microengineering*, vol. 4, pp. 157–171, 1994.
5. N.T. Nguyen, X.Y. Huang, and K.C. Toh, MEMS-Micropumps: A Review, *Journal of Fluids Engineering*, vol. 124, pp. 384–392, 2002.
6. E. Stemme and G. Stemme, Valveless Diffuser/Nozzle-Based Fluid Pump, *Sensors and Actuators A*, vol. 39, pp. 159–167,1993.
7. S. Matsumoto, A. Klein, and R. Maeda, Development of Bi-directional Valve-less Micropump for Liquid, Twelfth IEEE International Conference on MEMS, MEMS'99, pp. 141–146, Orlando, FL, January 17–21, 1999.
8. J. Tsai, L., Lin, A Thermal-Bubble-Actuated Micro Nozzle-Diffuser Pump, *Journal of Microelectromechanical Systems*, vol. 11, pp. 665–671, 2002.
9. A. Glezer and M.G. Allen, Micromachined Synthetic Jet Actuators and Applications Thereof, U.S. patent number 6457654 B1, 2002.
10. B.L. Smith and A. Glezer, The Formation and Evolution of Synthetic Jets, *Physics of Fluids*, vol. 10(9), pp. 2281–2297, 1998.
11. D.J. Coe, M.G. Allen, B.L. Smith, and A. Glezer, Addressable Micromachined Jet Arrays, *Technical Digest: Transducers 95*, The 8th International Conference on Solid-State-Sensors and Actuators, and Eurosensors IX Stockholm, Sweden, June 25–29, pp. 329–332, 1995.
12. L.D. Karl, J.F. Cain, and A.W. Cary, Numerical Simulation of Synthetic Jet Actuators, AIAA Paper 97–1824, 28th AIAA Fluid Dynamics Conference, Snowmass Village, CO, June 29–July 2, 1997.
13. S.G. Mallinson, J.A. Reizes, G. Hong, and P.S. Westbury, Analysis of Hot-Wire Anemometry Data Obtained in a Synthetic Jet Flow, *Experimental Thermal and Fluid Science*, vol. 28, pp. 265–272, 2004.
14. N. Beratlis and M.K. Smith, Optimization of Synthetic Jet Cooling for Microelectronics Applications, Nineteenth Annual IEEE Semiconductor Thermal Measurement and Management Symposium, pp. 66–73, San Jose, CA, March 11–13, 2003.

15. D.S. Kercher, J.B. Lee, O. Brand, M.G. Allen, and A. Glezer, Microjet Cooling Devices for Thermal Management of Electronics, *IEEE Transactions on Components and Packaging Technologies*, vol. 26(2), pp. 359–366, 1998.
16. C. Lee, G. Hong, Q.P. Ha, and S.G. Mallinson, A Piezoelectrically Actuated Micro Synthetic Jet for Active Flow Control, *Sensor and Actuators A*, vol. 108, pp. 168–174, 2003.